An Improved Analytical Model for Carrier Multiplication Near Breakdown in Diodes

Raymond J. E. Hueting, *Senior Member, IEEE*, Anco Heringa, Boni K. Boksteen, *Member, IEEE*, Satadal Dutta, *Student Member, IEEE*, Alessandro Ferrara, *Student Member, IEEE*, Vishal Agarwal, and Anne Johan Annema, *Member, IEEE*

***Abstract*— The charge carrier contributions to impact ionization and avalanche multiplication are analyzed in detail. A closed-form analytical model is derived for the ionization current before the onset of breakdown induced by both injection current components. This model shows that the ratio of both injection current components affects the multiplication factor at relatively low fields before breakdown, but does not affect the reverse breakdown voltage. Furthermore, the model indicates that in case the ionization coefficients of electrons and holes are quite different in value, which depends upon the semiconductor material, the ionization coefficient of the charge carrier with the highest value can be extracted at those low fields. The one with the lowest value can be obtained by fitting the current close to breakdown. The model is compared and verified with TCAD simulations, and to some extent with experimental data, for silicon p-i-n diodes.**

***Index Terms*— Avalanche breakdown, avalanche diodes, impact ionization, multiplication.**

I. Introduction

IN HIGH-VOLTAGE and power applications, p-n junction diodes or Schottky diodes are utilized as rectifiers, and MOSFETs as switches or synchronous rectifiers [1], [2]. For these devices, the reverse (OFF-state) breakdown voltage (BV) is a key figure of merit. Impact ionization near or at breakdown also plays a crucial role for the functionality of other types of devices, such as avalanche photodiodes [3]–[5], avalanche light-emitting devices [6], and steep-subthreshold switches (e.g., I-MOS [7] and positive feedback FET [8]). For modeling of degradation in CMOS and power devices caused by hot carrier and parasitic bipolar effects, impact ionization is important as well [9], [10]. In particular, the (shape of the) impact ionization current density-voltage characteristics near or at breakdown is important for these types of devices. The effect of tunneling and avalanche breakdown in a p-n junction was derived earlier [11]. However, Hurkx *et al.* [11] mainly focused on the tunneling behavior of the total diode current, and did not investigate the impact of the charge carrier contributions on the impact ionization.

This paper presents a detailed analysis of impact ionization current leading to a comprehensive closed-form model that can be used to accurately describe impact ionization, (weak) avalanche effects, and breakdown effects. This model includes the effects of the so-called impact ionization coefficients and the injection currents of both charge carriers. To the best of our knowledge, the impact of both to the multiplication factor and consequently to the current has not been considered elsewhere [1], [2], [12].

In many semiconducting materials, such as silicon (Si) [13], silicon-carbide (SiC) [2], [14], and gallium-nitride (GaN) [14], [15], particularly one of the carriers (Si: electrons; SiC, GaN: holes) has a much higher impact ionization coefficient than the other. We show that weak avalanche effects can properly be modeled by solely including the charge carrier with the highest ionization coefficient, but that breakdown effects require the ionization of both types of charge carriers.

This paper, which only focuses on a local avalanche model (for more details or background information on non-local avalanche we refer to [16] and [17]), is outlined as follows. Section II presents a brief overview of the traditional theory of impact ionization [1], [2] needed for this paper. In Section III, we present the closed-form model. Then, in Section IV, we compare the results with TCAD simulations and experimental data applied to p-i-n diodes, followed by Section V in which we discuss the implications of the charge carrier contributions in weak avalanche and breakdown. Finally, Section VI summarizes the conclusions of this paper.

II. Basic Background

Fig. 1 schematically illustrates the space charge (or multiplication) region (SCR) of a semiconductor device in reverse bias operation. At a relatively low reverse bias voltage, the total current density J equals the sum of the injected electron current density J_{n0} and hole current density J_{p0}. Depending upon the type of device, each of these components can be

Manuscript received July 19, 2016; revised October 24, 2016; accepted November 15, 2016. Date of publication November 29, 2016; date of current version December 24, 2016. This work was supported in part by the Agentschap NL (Dutch Point-One Program), an agency of the Dutch Ministry of Economic Affairs, and in part by the Dutch Technology Foundation STW, an applied science division of NWO and the Technology Program of the Ministry of Economic Affairs. The review of this paper was arranged by Editor J. Mateos.

R. J. E. Hueting and S. Dutta are with the MESA+ Institute for Nanotechnology, University of Twente, 7500AE Enschede, The Netherlands (e-mail: r.j.e.hueting@utwente.nl).

A. Heringa, retired, was with NXP Semiconductors, 5656AG, Eindhoven, The Netherlands.

B. K. Boksteen was with the MESA+ Institute for Nanotechnology, University of Twente, 7500AE Enschede, The Netherlands. He is now with ABB Semiconductors, 5600 Lenzburg, Switzerland.

A. Ferrara was with the MESA+ Institute for Nanotechnology, University of Twente, 7500AE Enschede, The Netherlands. He is now with Nexperia, Manchester, Stockport, SK7 5BJ, U.K.

V. Agarwal and A. J. Annema are with the CTIT Institute, University of Twente, 7500AE Enschede, The Netherlands.

Color versions of one or more of the figures in this paper are available online at http://ieeexplore.ieee.org.

Digital Object Identifier 10.1109/TED.2016.2630083

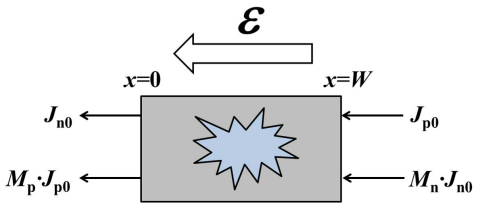

Fig. 1. Schematic of the SCR in a p(-i-)n or Schottky diode with the initial injection components of the current density, J_{n0} and J_{p0}, and the final components obtained through impact ionization, $M_p \cdot J_{p0}$, respectively $M_n \cdot J_{n0}$. Such a diode is present in most active devices. W represents the width of the SCR. The total current density $J = M_n(W) \cdot J_{n0} + J_{p0} = M_p(0) \cdot J_{p0} + J_{n0}$; $\mathscr{E}$ represents the electric field.

separately tuned changing the doping, contacts, or materials. When we increase the reverse bias voltage, the charge carriers in the SCR are accelerated by the electric field $\mathscr{E}$. For a high $\mathscr{E}$, the charge carriers are accelerated, such that they excite, due to scattering in the semiconductor lattice, electron–hole pairs. This electron–hole pair generation is called impact ionization, and it causes an increase in both current components and each of these components is separated due to the electric field (see Fig. 1). This increase can be described by the so-called multiplication factors M_n and M_p, which in turn depend on the impact ionization coefficients of both electrons and holes, respectively, α_n and α_p. These $\mathscr{E}$-dependent coefficients represent the number of generated electron–hole pairs per unit length caused by an electron and hole current, respectively.

Considering only generation of charge carriers through impact ionization within an infinitesimal small distance dx in the SCR, the change in electron current density can be written as [1]

$$\frac{dJ_n}{dx} = \alpha_n \cdot J_n + \alpha_p \cdot J_p. \tag{1}$$

For the electron and hole current density, $J_n = -q \cdot n \cdot \upsilon_n$, respectively, $J_p = q \cdot p \cdot \upsilon_p$, where q is the elementary charge and υ_n and υ_p are the electron and hole drift velocities, respectively. In this paper for simplicity reasons, it is assumed that $-\upsilon_n = \upsilon_p = \upsilon_{\text{sat}}$, where υ_{sat} is the saturation velocity for electrons (in Si this is $\sim 10^7$ cm/s). The carriers reach υ_{sat} at relatively high fields [typically $\mathscr{E}(x) \gtrsim 10^4$ V/cm].

Similarly

$$\frac{dJ_p}{dx} = -\alpha_n \cdot J_n - \alpha_p \cdot J_p. \tag{2}$$

Hence, in the whole device, the total current density J is constant. As the next step, we derive relations for the carrier multiplication factors M_n and M_p.

III. Closed-Form Model

Taking the ionization of both carriers into account results in relatively complicated relations. Earlier [1], some relations for the multiplication factor had been derived for this case using one injection current component only. In other work, several relations for the "average" multiplication factor were derived [2], [12]. In the closed-form model presented in this paper, we solve (1) and (2) including both J_{n0} and J_{p0} as described in the Appendix. The relations shown herein could also be obtained following [1] assuming the boundary conditions presented in Fig. 1.

The main relations derived in the Appendix, needed for this paper, describe the electron current density as

$$J_n(x) = -\int_0^x c_p \cdot \exp\left(-\int_{x'}^W (\alpha_n - \alpha_p) dx''\right) dx' + J_{n0} \tag{3}$$

with

$$c_p = -\alpha_n \cdot M_n(W) \cdot J_{n0} - \alpha_p \cdot J_{p0} \tag{4}$$

and describe the electron multiplication factor at the edge of the SCR as

$$M_n(W) = \frac{1 + k \cdot \int_0^W \alpha_p \cdot \exp\left(-\int_x^W (\alpha_n - \alpha_p) dx'\right) dx}{1 - \int_0^W \alpha_n \cdot \exp\left(-\int_x^W (\alpha_n - \alpha_p) dx'\right) dx} \tag{5}$$

with $k = J_{p0}/J_{n0}$ is the injection current ratio.

Similarly, for holes, it was derived that

$$J_p(x) = \int_x^W c_n \cdot \exp\left(\int_0^{x'} (\alpha_n - \alpha_p) dx''\right) dx' + J_{p0} \tag{6}$$

with

$$c_n = \alpha_n \cdot J_{n0} + \alpha_p \cdot M_p(0) \cdot J_{p0} \tag{7}$$

and with the hole multiplication factor described as

$$M_p(0) = \frac{1 + \frac{1}{k} \cdot \int_0^W \alpha_n \cdot \exp\left(\int_0^x (\alpha_n - \alpha_p) dx'\right) dx}{1 - \int_0^W \alpha_p \cdot \exp\left(\int_0^x (\alpha_n - \alpha_p) dx'\right) dx}. \tag{8}$$

Hence, for the total current density, it follows that $J = M_n(W) \cdot J_{n0} + J_{p0} = M_p(0) \cdot J_{p0} + J_{n0}$ (see also Fig. 1). Depending on k for a wide bias range, the impact ionization current density can be described as $J_{\text{ii}} = M_n(W) \cdot J_{n0}$ ($k \geq 1$), or $J_{\text{ii}} = M_p(0) \cdot J_{p0}$ ($k \leq 1$), as is discussed in Section V.

The denominators in (5) and (8) are the familiar relations needed to obtain the relation for avalanche, i.e., $M_n(W) \to \infty$ or $M_p(0) \to \infty$ [1], [5], [13], [16], [18], [19]. These basically induce the positive feedback needed for a sharp rise in current during avalanche. However, the numerators in both equations are different from what has been reported earlier. Here, each separate component, J_{n0} and J_{p0}, has been included and plays a role in the multiplication factor as well.

For the special case, $\alpha_n = \alpha_p = \alpha$, such as in gallium-phosphide (GaP) [1], (5) and (8) simplify to

$$M_n(W) = \frac{1 + k \cdot \int_0^W \alpha dx}{1 - \int_0^W \alpha dx} \tag{9}$$

and

$$M_p(0) = \frac{1 + \frac{1}{k} \cdot \int_0^W \alpha dx}{1 - \int_0^W \alpha dx} \tag{10}$$

respectively.

In Section IV, we also consider the situation where $\alpha_p = 0$, a simplification that implies that extra holes are solely generated by electron collisions and a hole current $J_p > J_{p0}$ is formed. This case is interesting since in semiconducting

materials such as Si [13], [20], α_p is typically one order of magnitude lower than α_n (depending on the applied field). For materials such as SiC or GaN $\alpha_p \gg \alpha_n$ [2], [14], [15], and for such materials, one could be tempted to neglect α_n.

When α_p is set to zero, (8) reduces to

$$M_p(0) = \frac{1}{k} \cdot \int_0^W \alpha_n \cdot \exp\left(\int_0^x \alpha_n dx'\right) dx + 1. \quad (11)$$

However, obtaining a simple relation for $M_n(W)$ from (5) considering $\alpha_p = 0$ is more difficult. Considering $\alpha_p = 0$ for a constant field distribution, *i.e.*, p-i-n diode, (5) reduces to [21]

$$M_n(W) = \exp(\alpha_n \cdot W). \quad (12)$$

IV. Application to p-i-n Diodes

In this paper, we apply the results to p-i-n diodes. This is because in reverse biased p-i-n diodes $\mathscr{E}(x) = \mathscr{E}$, and therefore, $\alpha_{p,n}$ is spatially constant. This constant field results in more simple and closed form analytical relations compared with the ones for a conventional p-n junction diode. Moreover, the assumption of the constant v_{sat} is physically more sound in a p-i-n diode because of the constant (high) field, which obviously does not hold in the SCR of a conventional p-n junction diode. In addition, such a constant field can also be obtained when adopting the RESURF, i.e., REduced SURface field, effect [22]–[25] commonly used in power devices.

A. Ionization Models

For analyzing the impact ionization and avalanche breakdown, we incorporate the traditional Chynoweth relation [26] for the impact ionization coefficients

$$\alpha_{p,n} = A_{p,n} \cdot \exp\left(-\frac{B_{p,n}}{|\mathscr{E}|}\right) \quad (13)$$

with Si parameter values reported in [16] and [27] obtained from experimental data, which are widely used in both industry and academia: $A_n = 7.03 \times 10^5$ 1/cm, $B_n = 1.236 \times 10^6$ V/cm, $A_p = 6.71 \times 10^5$ 1/cm, and $B_n = 1.396 \times 10^6$ V/cm.

In the literature, the denominator of (9) and (10) is often used for calculating the BV (i.e., for $\int_0^W \alpha dx = 1$) when considering Fulop's approximation [2], [28]

$$\alpha = A_F \cdot |\mathscr{E}|^7 \quad (14)$$

with $A_F = 1.8 \cdot 10^{-35}$ cm$^6 \cdot$ V^{-7} as a fit parameter for Si.

Fig. 2 shows W versus calculated BV values obtained from the model in which Chynoweth's relation, i.e., (5) and (8) with (13), has been incorporated. For comparison, the values from the model in which Fulop's approximation (*i.e.*, (9), (10), and (14)) has been incorporated are shown as well. For convenience sake for the remainder of this paper, we just refer to "Chynoweth" and "Fulop's approximation" when using the model in which Chynoweth's relation, respectively, Fulop's approximation has been incorporated. In Si p-i-n diodes, for BV $<$ 100 V, the results obtained from Fulop's approximation are comparable with those obtained with Chynoweth's relation. For BV $\gtrsim$ 100 V, Fulop's approximation shows somewhat lower BV values ($\sim$15%) for the same W. Note

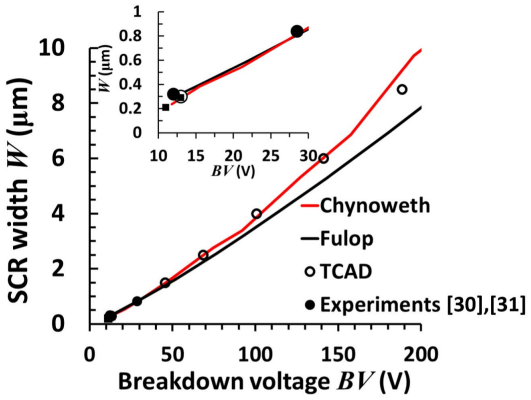

Fig. 2. Calculated BV values in Si p-i-n diodes obtained by using Fulop's approximation (14) in our analytical model (see (9) and (10)), i.e., $\alpha_n = \alpha_p = \alpha$, and by using Chynoweth's relation (13) with A_n = 7.03 x 10^5 1/cm, B_n = 1.236 x 10^6 V/cm, A_p = 6.71 x 10^5 1/cm, and B_n = 1.396 x 10^6 V/cm. TCAD simulations [32] with parameter Si values from [16] and [27] are shown for comparison. The experimental data have been obtained from [30] and [31]. Inset: zoomed-in view of the data for lower BV values.

that van Dalen *et al.* [29] found that for high voltage Si devices with dominating electron multiplication, the parameter A_F should be increased to 10^{-34} cm$^6 \times$ V^{-7} so that Fulop's model is in good agreement with their experimental M_n data. For comparison in Fig. 2, we also included experimental data obtained from [30] and [31] and TCAD simulations [32], showing good agreement.

B. Results

As an example, we further focus on two Si p-i-n diodes in reverse bias, with $W = 0.3$ and 6 μm, respectively.

Using the models, i.e., Chynoweth and Fulop's approximation, we provide a further insight of the devices. Fig. 3 shows $J_p(x)$ and $J_n(x)$ near breakdown, in this case 12 V (BV $\approx$ 13 V), in the SCR for the 0.3-μm device. For the calculations, we considered Chynoweth with $\alpha_p = 0$ and $\alpha_p \neq 0$ (see (3)–(8) and (13)), where $J_{n0} = 200$ nA/cm^2: 1) a low $J_{p0} = 200$ nA/cm^2 (i.e., $k = J_{p0}/J_{n0} = 1$) and 2) a relatively high $J_{p0} = 20$ μA/cm^2 (i.e., $k = 100$) are assumed. The results show that for case 1), the current density levels are comparable irrespective the value of α_p, whereas for a higher J_{p0}, these levels start increasing for the case when $\alpha_p \neq 0$. As is discussed further in this section, this appears to indicate that the hole contribution should be included despite the relatively low α_p [5].

Fig. 4 shows $J_p(x)$ and $J_n(x)$ near the breakdown condition for both devices obtained from the model (with Chynoweth) compared with TCAD simulations [32]. In the TCAD simulations, we adopt the same $\alpha_{p,n}$ parameters as used in our analytical model. The discrepancy between the TCAD simulations and the model in Fig. 4 could be attributed to differences in saturation velocity between electrons and holes, not taken into account in the model.

For power devices, BV is a key figure of merit. For some types of devices, not only the actual BV value but also the (shape of the) J_{ii} or J as a function of the voltage near or at breakdown is important, as stated in Section I.

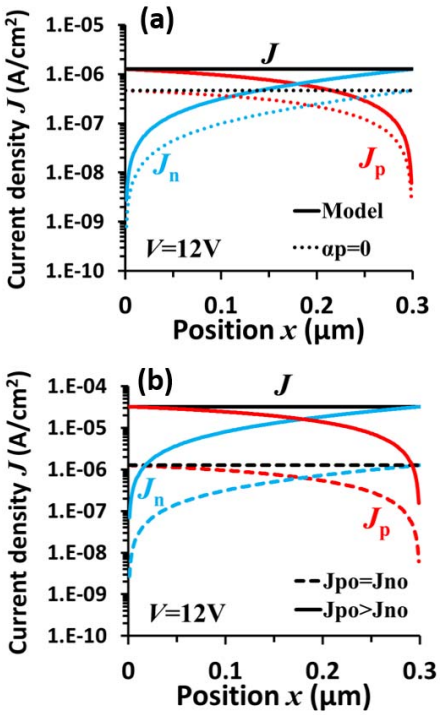

Fig. 3. Calculated current density distributions inside the 0.3-μm-wide SCR of a Si p-i-n diode obtained from the model with (a) $\alpha_p = 0$ and the Chynoweth relations ($\alpha_{p,n} \neq 0$) for J_{n0} = 200 nA/cm^2 and (b) model for J_{n0} = 200 nA/cm^2, and varying J_{p0} = 200 nA/cm^2 (k = 1) and J_{p0} = 20 μA/cm^2 (k = 100).

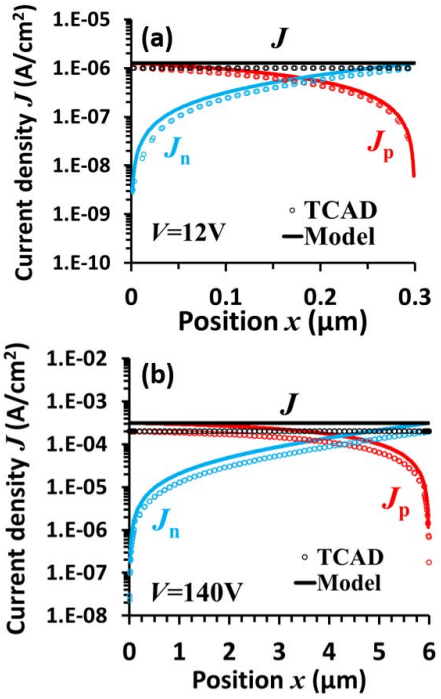

Fig. 4. Current density distributions inside an Si p-i-n diode with (a) 0.3-μm-wide SCR ($J_{n0} = J_{p0}$ = 200 nA/cm^2) and (b) 6-μm-wide SCR ($J_{n0} = J_{p0}$ = 4.8 μA/cm^2) obtained from the model including Chynoweth's relation, compared with TCAD simulations.

In Fig. 5, J is plotted against the applied bias for both p-i-n diodes when $J_{n0} = J_{p0}$. Here, we employed the model for $\alpha_p = 0$, Chynoweth ($\alpha_{p,n} \neq 0$), and Fulop's approximation for comparison. Prior to breakdown, similar results are obtained for J irrespective the value of α_p indicating that α_p is less important for low fields when $\alpha_n \cdot W \gg 1$ and $\alpha_p \cdot W \ll 1$ [21]. However, at the onset of breakdown, the model shows a clear and dramatic increase in current when adopting Chynoweth, as in the TCAD simulations. When $\alpha_p = 0$, the model shows a weaker slope ("weak avalanche") where the BV is not well defined. It is clear that closer to the breakdown condition, J is to a great extent also determined by α_p, while at lower voltages $J \approx J_n$. This indicates that in case of Si, α_n can be obtained at low reverse fields (by fitting e.g., the backgate or substrate current of an nMOS). After extracting α_n at those low fields, α_p can be obtained only by fitting the current near breakdown condition. As stated earlier, Fulop's approximation shows a discrepancy in the BV.

We also investigate the effect of J_{p0} on the J_{ii}–V curves for both devices utilizing the model (including Chynoweth's relation, see Fig. 6). In case of $J_{p0} \gg J_{n0}$ ($1/k \rightarrow 0$, (8)) in both devices initially, J_p is determined by J_{p0} but near breakdown by J_n as well. In this case when using the traditional M_p [1], the J_n curve would not have been obtained. Rather, the shape of the J_n–V curve, which is actually describing J_{ii}, can be obtained with the model. Likewise, when using the traditional M_n [1], hence $k \rightarrow 0$ (or $J_{p0} \ll J_{n0}$) in (5) of the model, the J_n–V curve would have been obtained only, and not the J_p–V curve. In other words, before and near breakdown, the model adequately describes J_{ii} because of the incorporation of the injection current densities for both charge carriers.

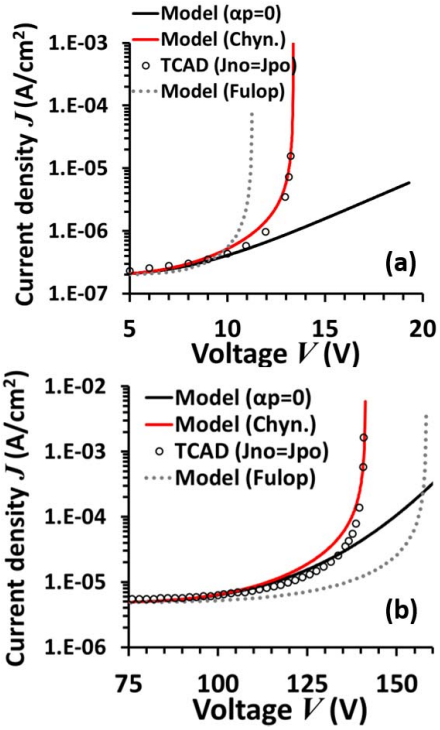

Fig. 5. Total current density J against the voltage for two Si p-i-n diodes. (a) 0.3-μm diode ($J_{n0} = J_{p0}$ = 200 nA/cm^2) and (b) 6-μm diode ($J_{n0} = J_{p0}$ = 4.8 μA/cm^2) obtained from the model for $\alpha_p = 0$, Chynoweth relations, Fulop's approximation, and TCAD simulations.

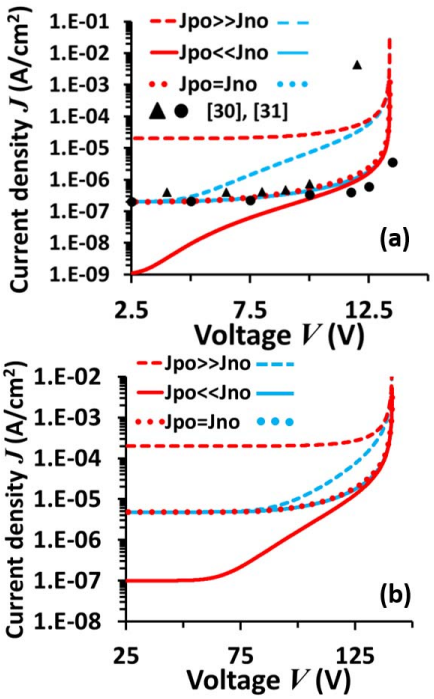

Fig. 6. J_n and J_p against the voltage for two Si p-i-n diodes using the model with Chynoweth's relations. (a) 0.3-μm diode (J_{n0} = 200 nA/cm^2) and (b) 6-μm diode (J_{n0} = 4.8 μA/cm^2), and varying J_{p0}: $J_{p0} = J_{n0}$, $J_{p0} \gg J_{n0}$, and $J_{p0} \ll J_{n0}$. The experimental data have been obtained from [30] and [31].

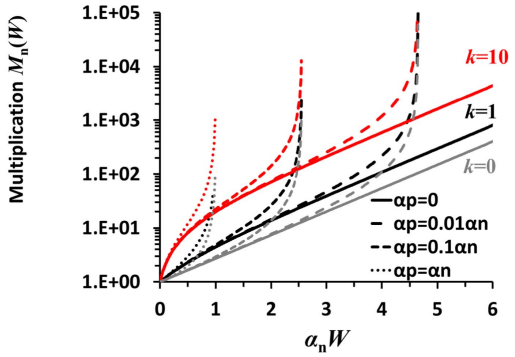

Fig. 7. Multiplication factor as a function of $\alpha_n \cdot W$ for a constant field for various ratios $\gamma = \alpha_p/\alpha_n$ = 0, 0.01, 0.1, and 1, and injection current ratios $J_{p0}/J_{n0} = k$ = 0, 1, and 10.

V. Discussion

Fig. 7 shows for a reverse biased p-i-n diode M_n, given by (5), as a function of $\alpha_n \cdot W$ for some α_p values (0, 0.01·α_n, 0.1·α_n, and α_n). As stated at the end of Section II, M_n never reaches infinity when $\alpha_p = 0$, so no avalanche breakdown occurs in this case. Furthermore, at low M_n, all the curves coincide (all have the same α_n), as observed in our previous results. In particular, the $k = J_{p0}/J_{n0}$ value variation shows the impact of the injection on M_n, in comparison with more traditional relations [1] (k =0). Therefore, for low fields, α_p is not important in Si. The injection current ratio k shifts the curves vertically, and hence, BV is not changed, only M_n. When one fits the BV only with α_n, the slope of the curves is modified. The strong curvature for cases with $\alpha_p \neq 0$ occurs at $M_n \approx (k+1) \cdot \alpha_n/\alpha_p$.

In summary, despite the large difference between α_p and α_n, the model is needed to have a good description for J_{ii} at the price of the complexity. As reported earlier [27], care has to be taken when fitting α_n and α_p from BV measurements only, since these will not be suited for calculating the multiplication factor not taking into account properly $k = J_{p0}/J_{n0}$ and the ratio α_p/α_n.

VI. Conclusion

Relations for the multiplication factor have been presented considering both charge carriers. It is shown that when considering the ionization coefficient of solely one charge carrier, only weak avalanche is obtained. On the other hand, avalanche breakdown is obtained when considering the ionization coefficients for both charge carriers, irrespective the differences in the magnitude of those. When focusing on the impact ionization current near or at breakdown, the ionization coefficients and injection currents of both charge carriers should be incorporated.

Appendix

In prior literature [1], [2], the injection current contributions for only one type of charge carrier are used for determining the multiplication factors. Generally, J_{n0} (J_{p0}) is ignored for determining the hole (electron) multiplication factor (so, $J_{p0} = 0$ in (5) and (9), and $J_{n0} = 0$ in (8) and (10)).

In this section, we come up with a new approach for determining the multiplication factors when both J_{p0} and J_{n0} are included. Since J is constant, (1) can be written as

$$\frac{d^2 J_n}{dx^2} = (\alpha_n - \alpha_p) \cdot \frac{dJ_n}{dx}.$$

Similarly, we obtain from (2)

$$\frac{d^2 J_p}{dx^2} = (\alpha_n - \alpha_p) \cdot \frac{dJ_p}{dx}.$$

Hence

$$\ln\left(\frac{dJ_n}{dx}\right) + c = \int_0^x (\alpha_n - \alpha_p) dx'$$

where the boundary value $c = -\ln(c_n) = -\ln((dJ_n)/(dx)|_{x=0})$. Then

$$\frac{dJ_n(x)}{dx} = c_n \cdot \exp\left(\int_0^x (\alpha_n - \alpha_p) dx'\right) \quad (15)$$

and

$$J_n(x) = \int_0^x c_n \cdot \exp\left(\int_0^{x'} (\alpha_n - \alpha_p) dx''\right) dx' + c \quad (16)$$

with $c = J_n(0)$.

Similarly

$$\frac{dJ_p(x)}{dx} = c_p \cdot \exp\left(-\int_x^W (\alpha_n - \alpha_p) dx'\right) \quad (17)$$

which results in

$$J_p(x) = \int_W^x c_p \cdot \exp\left(-\int_{x'}^W (\alpha_n - \alpha_p) dx''\right) dx' + c'. \quad (18)$$

Now, we need all integration constants of (15)–(18). Substituting (15) and (17) and knowing that J is spatially constant gives

$$-\frac{c_n}{c_p} = \frac{\exp\left(-\int_x^W (\alpha_n - \alpha_p)dx'\right)}{\exp\left(\int_0^x (\alpha_n - \alpha_p)dx'\right)} = \exp\left(-\int_0^W (\alpha_n - \alpha_p)dx'\right) \tag{19}$$

which hence is also spatially constant.

Further with (1) and (2), we can also write (see Fig. 1)

$$\frac{dJ_n}{dx}\,|_{x=0} = c_n = \alpha_n \cdot J_{n0} + \alpha_p \cdot M_p(0) \cdot J_{p0} \tag{20}$$

and similarly

$$\frac{dJ_p}{dx}\,|_{x=W} = c_p = -\alpha_n \cdot M_n(W) \cdot J_{n0} - \alpha_p \cdot J_{p0}. \tag{21}$$

Therefore, it can be derived that

$$J_n(W) = J_{n0} \cdot M_n(W) = -\int_0^W c_p \cdot \exp\left(-\int_x^W (\alpha_n - \alpha_p)dx'\right)dx + c \tag{22}$$

and

$$J_n(0) = J_{n0} = c. \tag{23}$$

Substituting the values of c_p and c from (21) and (23) into (22), and after some rearranging, we obtain for the electron multiplication factor

$$M_n(W) = \frac{1 + \frac{J_{p0}}{J_{n0}} \cdot \int_0^W \alpha_p \cdot \exp\left(-\int_x^W (\alpha_n - \alpha_p)dx'\right)dx}{1 - \int_0^W \alpha_n \cdot \exp\left(-\int_x^W (\alpha_n - \alpha_p)dx'\right)dx}$$

as stated in (5). Similarly, for the hole contribution, we can state

$$J_p(0) = M_p(0) \cdot J_{p0} = \int_0^W c_n \cdot \exp\left(\int_0^x (\alpha_n - \alpha_p)dx'\right)dx + c' \tag{24}$$

and

$$J_p(W) = J_{p0} = c'. \tag{25}$$

Therefore, for the hole multiplication factor, we obtain

$$M_p(0) = \frac{1 + \frac{J_{n0}}{J_{p0}} \cdot \int_0^W \alpha_n \cdot \exp\left(\int_0^x (\alpha_n - \alpha_p)dx'\right)dx}{1 - \int_0^W \alpha_p \cdot \exp\left(\int_0^x (\alpha_n - \alpha_p)dx'\right)dx}$$

as stated in (8). Equations (3) and (6) are obtained from (21) and (22), respectively, (20) and (24).

REFERENCES

[1] S. M. Sze and K. K. Ng, *Physics of Semiconductor Devices*, 3rd ed. Hoboken NJ, USA: Wiley, 2007.

[2] B. J. Baliga, *Fundamentals of Power Semiconductor Devices*. New York, NY, USA: Springer, 2008.

[3] W. J. Kindt, "Geiger mode avalanche photodiode arrays," Ph.D. dissertation, Dept. Elect. Eng., Delft Univ. Technol., Delft, The Netherlands, 1999.

[4] D. Renker, "Geiger-mode avalanche photodiodes, history, properties and problems," *Nucl. Instrum. Methods Phys. Res. A, Accel. Spectrom. Detect. Assoc. Equip.*, vol. 567, no. 1, pp. 48–56, Nov. 2006.

[5] G. E. Stillman and C. M. Wolfe, "Avalanche photodetectors," in *Semiconductors Semimetals, Infrared Detectors II*, vol. 12, R. K. Willardson and A. C. Beer, Eds. New York, NY, USA: Academic, 1977, p. 304.

[6] L. W. Snyman, M. du Plessis, and E. Bellotti, "Photonic transitions (1.4 eV–2.8 eV) in silicon p^+np^+ injection-avalanche CMOS LEDs as function of depletion layer profiling and defect engineering," *IEEE J. Quantum Electron.*, vol. 46, no. 6, pp. 906–919, Jun. 2010.

[7] K. Gopalakrishnan, P. B. Griffin, and J. D. Plummer, "I-MOS: A novel semiconductor device with a subthreshold slope lower than kT/q," in *IEDM Tech. Dig.*, Dec. 2002, pp. 289–292.

[8] C. W. Cheung, C. Shin, C. Hu, and T. J. K. Liu, "Feedback FET: A novel transistor exhibiting steep switching behavior at low bias voltages," in *IEDM Tech. Dig.*, Dec. 2008, pp. 1–4.

[9] E. Takeda and N. Suzuki, "An empirical model for device degradation due to hot-carrier injection," *IEEE Electron Device Lett.*, vol. EDL-4, no. 4, pp. 111–113, Apr. 1983.

[10] P. Moens, G. Van den bosch, and G. Groeseneken, "Hot-carrier degradation phenomena in lateral and vertical DMOS transistors," *IEEE Trans. Electron Devices*, vol. 51, no. 4, pp. 623–628, Apr. 2004.

[11] G. A. M. Hurkx, H. C. de Graaff, W. J. Kloosterman, and M. P. G. Knuvers, "A new analytical diode model including tunneling and avalanche breakdown," *IEEE Trans. Electron Devices*, vol. 39, no. 9, pp. 2090–2098, Sep. 1992.

[12] R. J. McIntyre, "Multiplication noise in uniform avalanche diodes," *IEEE Trans. Electron Devices*, vol. ED-13, no. 1, pp. 164–168, Jan. 1966.

[13] R. Van Overstraeten and H. De Man, "Computer calculation of ionisation rates in silicon for a diffused junction," *Electron. Lett.*, vol. 3, no. 10, pp. 469–471, 1967.

[14] T. P. Chow *et al.*, "SiC and GaN bipolar power devices," *Solid-State Electron.*, vol. 44, no. 2, pp. 277–301, Feb. 2000.

[15] I. H. Oğuzman, E. Belloti, K. F. Brennan, J. Kolník, R. Wang, and P. P. Ruden, "Theory of hole initiated impact ionization in bulk zincblende and wurtzite GaN," *J. Appl. Phys.*, vol. 81, no. 12, pp. 7827–7834, 1997.

[16] W. Maes, K. De Meyer, and R. Van Overstraeten, "Impact ionization in silicon: A review and update," *Solid-State Electron.*, vol. 33, no. 6, pp. 705–718, 1990.

[17] J. W. Slotboom, G. Streutker, M.J. van Dort, P. H. Woerlee, A. Pruijmboom, and D. J. Gravesteijn, "Non-local impact ionization in silicon devices," in *IEDM Tech. Dig.*, Dec. 1991, pp. 127–130.

[18] S. L. Miller, "Ionization rates for holes and electrons in silicon," *Phys. Rev.*, vol. 105, pp. 1246–1249, Feb. 1957.

[19] J. L. Moll and R. Van Overstraeten, "Charge multiplication in silicon P-N junctions," *Solid-State Electron.*, vol. 6, no. 2, pp. 147–157, 1963.

[20] B. K. Boksteen, A. Heringa, A. Ferrara, P. G. Steeneken, J. Schmitz, and R. J. E. Hueting, "Electric field and interface charge extraction in field-plate assisted RESURF devices," *IEEE Trans. Electron Devices*, vol. 62, no. 2, pp. 622–629, Feb. 2015.

[21] M. Levinshtein, J. Kostamovaara, and S. Vainshtein, *Breakdown Phenomena in Semiconductors and Semiconductor Devices* (Selected Topics in Electronics and Systems), vol. 36. NJ, USA: World Scientific, 2005.

[22] J. A. Appels and H. M. J. Vaes, "High voltage thin layer devices (RESURF devices)," in *IEDM Tech. Dig.*, Dec. 1979, pp. 238–241.

[23] S. Merchant, "Analytical model for the electric field distribution in SOI RESURF and TMBS structures," *IEEE Trans. Electron Devices*, vol. 46, no. 6, pp. 1264–1267, Jun. 1999.

[24] T. Fujihira, "Theory of semiconductor superjunction devices," *Jpn. J. Appl. Phys.*, vol. 36, no. 10, pp. 6254–6262, Oct. 1997.

[25] A. Ferrara, B. K. Boksteen, R. J. E. Hueting, A. Heringa, J. Schmitz, and P. G. Steeneken, "Ideal RESURF geometries," *IEEE Trans. Electron Devices*, vol. 62, no. 10, pp. 3341–3347, Oct. 2015.

[26] A. G. Chynoweth, "Ionization rates for electrons and holes in silicon," *Phys. Rev.*, vol. 109, no. 5, pp. 1537–1540, 1958.

[27] R. Van Overstraeten and H. De Man, "Measurement of the ionization rates in diffused silicon *p-n* junctions," *Solid-State Electron.*, vol. 13, no. 5, pp. 583–608, 1970.

[28] W. Fulop, "Calculation of avalanche breakdown voltages of silicon P-N junctions," *Solid-State Electron.*, vol. 10, no. 1, pp. 39–43, 1967.

[29] R. van Dalen, A. Heringa, P. W. M. Boos, A. B. van der Wal, and M. J. Swanenberg, "Using multiplication to evaluate HCI degradation in HV-SOI devices," in *Proc. Int. Symp. Power Semiconductor Devices ICs (ISPSD)*, Jun. 2010, pp. 89–92.

[30] C. H. Tan *et al.*, "Avalanche multiplication and noise in submicron Si p-i-n diodes," *Proc. SPIE*, vol. 3953, pp. 95–102, Mar. 2000.
[31] P. Agarwal, M. J. Goossens, V. Zieren, E. Aksen, and J. W. Slotboom, "Impact ionization in thin silicon diodes," *IEEE Electron Device Lett.*, vol. 25, no. 12, pp. 807–809, Dec. 2004.
[32] *ATLAS Device Simulation Software, V.5.21.3.C*, Silvaco Inc., Santa Clara, CA, USA, 2015.

Raymond J. E. Hueting (S'94–M'98–SM'06) received the M.Sc. (*cum laude*) and Ph.D. degrees in electrical engineering from the Delft University of Technology, Delft, The Netherlands.

In 2005, he joined the Semiconductor Components Group, University of Twente, Enschede, The Netherlands, where he was involved in semiconductor device physics and modeling.

Anco Heringa received the M.Sc. degree in technical physics from the University of Groningen, Groningen, The Netherlands, in 1977.

He was a Consultant in process/device modeling with Philips, Eindhoven, The Netherlands, until 2002. He was with NXP, Eindhoven, where he was involved in integrated high-voltage devices until his retirement in 2014.

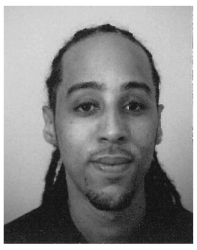

Boni K. Boksteen (S'10–M'16) received the M.Sc. (*cum laude*) and Ph.D. degrees in electrical engineering from the University of Twente, Enschede, The Netherlands.

He joined ABB Semiconductors, Lenzburg, Switzerland.

Satadal Dutta (S'15) received the B.Tech. degree (Hons.) in electronics and electrical communication engineering and the M.Tech. degree in microelectronics and VLSI from IIT Kharagpur, Kharagpur, India, in 2013. He is currently pursuing the Ph.D. degree with the Group of Semiconductor Components, MESA+ Institute for Nanotechnology, University of Twente, Enschede, The Netherlands.

Alessandro Ferrara (S'12) received the master's (*cum laude*) degree in electronic engineering from the Federico II University of Naples, Italy, in 2011, and the Ph.D. (*cum laude*) degree from the University of Twente, Enschede, The Netherlands.

He joined Nexperia, Manchester, U.K.

Vishal Agarwal received the bachelor's and master's degrees in electrical engineering from IIT Kanpur, Kanpur, India, in 2011. He is currently pursuing the Ph.D. degree with the Integrated Circuit Design Group, University of Twente, Enschede, The Netherlands.

From 2011 to 2014, he was with Intel Technology India Pvt. Ltd., Bengaluru, India.

Anne Johan Annema (M'00) received the M.Sc. and Ph.D. degrees from the University of Twente, Enschede, The Netherlands, in 1990 and 1994, respectively.

Since 2000, he has been with the Integrated Circuits Design Group, University of Twente, where he has been involving in device physics, analog, RF and mixed-signal electronics, and their joint feasibility aspects.